

Effects of Intrauterine Air Bubbles on Embryonic Development in Mice

Hua Li,^{1,†} Rongyan Zhou,^{1,†} Yimeng Li,² Ruonan Liu,¹ Yanping Miao,¹ Bin Zhang,¹ Xinglong Wu,³ Shu Zhang,³ Fuchou Tang,³ and Xiangyun Li^{1,*}

During murine embryo transfer, air bubbles frequently are loaded with embryos into the transfer catheter, but the role of air bubbles on embryonic development is unclear. This study shows that intrauterine air disrupted embryo spacing, induced decidualoma, and impaired postimplantation development. RNA sequencing showed that the gene expression profile of air-induced decidualoma differed significantly from that of embryo-induced decidua but is similar to tetraploid-induced decidualoma. A subset of 33 common genes was upregulated in the embryo-induced decidua compared with air- or tetraploid-induced decidualoma. These data suggest that the inner cell mass (ICM) plays a key role in regulating decidualization and that the trophoblast is an intermediate that relays ICM-derived signals to other target cells. Our results may provide an innovative approach for detecting the developmental status of embryos in human reproductive medicine.

Abbreviation: FPKM, fragments per kilobase of transcript per million fragments mapped; Gapdh, glyceraldehyde 3-phosphate dehydrogenase; GO, gene ontology; GV, germinal vesicle; TCET, transcervical embryo transfer; TGC, trophoblast giant cell

DOI: 10.30802/AALAS-JAALAS-18-000031

Murine embryo transfer is the final and key step needed to produce offspring after in vitro fertilization or a transgenic procedure and is accomplished surgically or by transferring embryos into the oviduct or uterine horn of a pseudopregnant mouse. During the transfer of embryos into the uterine horn, air bubbles frequently are loaded with embryos into the transfer catheter.²⁶ However, the role of air bubbles on murine embryonic development is unclear. In addition, the issue has not been addressed in regard to embryo transfer procedures for humans and other animals.^{5,31}

In mice, the onset of pregnancy is heralded by the attachment of an embryo to the luminal epithelium and its penetration into the stroma of the endometrium. In response to the steroid hormones estrogen and progesterone, the stromal cells surrounding the implantation chamber undergo a remarkable transformation. This process, known as decidualization, is an essential prerequisite for successful implantation.³² However, an implanting embryo is not absolutely required for endometrial decidualization.¹² Decidualization can occur in response to an artificial stimulus, such as small beads or droplets of oil injected into the uterine lumen.^{2,24} The endometrial tissue that forms in response to an artificial decidualogenic stimulus is called a decidualoma to distinguish it from naturally induced decidua. Air bubbles reportedly can induce decidualization in mice, rats, and hamsters,^{11,28} but whether air-induced decidualization disturbs decidual gene expression, implantation, or embryonic development is unclear currently.

Materials and Methods

Animals. Female (age, 8 to 12 wk) and male (age, 3 to 10 mo) CD1 mice (Beijing Vital River Laboratory Animal Technology, Beijing, China) were housed under constant environmental conditions (25 ± 1 °C; relative humidity, 40% to 60%; lights on, 0600 to 1800) at our institutional animal facility. Quarterly sentinel surveillance was used to screen for a wide range of pathogens, including epizootic diarrhea of infant mice, mouse hepatitis virus, mouse norovirus, mouse parvovirus 1 and 2, *Mycoplasma pulmonis*, pneumonia virus of mice, Sendai virus, *Helicobacter* spp., fur mites, and pinworms. All results from sentinel mice tested negative throughout this study. Mice received autoclaved feed (Beijing Vital River) and reverse-osmosis–deionized water without restriction. Mice were housed in polycarbonate microisolation caging with autoclaved hardwood bedding (Beijing Vital River). Autoclaved environmental enrichment was provided weekly to all mice in the form of 5-cm squares of cotton batting that could be shredded to form nests. All procedures in this study were approved by Hebei Agricultural University Laboratory Animal Care and Use Committee.

Air-induced decidualization in pseudopregnant mice. Female CD1 mice were mated with vasectomized males. The next morning the female mice were examined for vaginal plugs, and the plug-positive females were considered to be at day 0.5 of pseudopregnancy. On day 3.5, between 1500 to 1700, air was infused into the lumen of a single uterine horn (stimulated) by using transcervical embryo transfer (TCET) devices (Zhengmu Biotechnology, Baoding, China); the contralateral horn served as a control (nonstimulated).⁷ On day 7.5, the mice were killed by cervical dislocation, and uterine horns were dissected. The extent of decidualization was evaluated by separately weighing the stimulated and nonstimulated uterine horns. The dilated uterine horn that had a nonbeaded appearance was considered to be the horn infused with air. The difference in weight between the 2 horns was taken as an estimate of the response to the air

Received: 19 Mar 2018. Revision requested: 12 Apr 2018. Accepted: 07 May 2018.

¹College of Animal Science and Technology, Hebei Agricultural University, Baoding, Hebei, China; ²School of Basic Medical Science, Hebei Medical University, Shijiazhuang, Hebei, China; ³Beijing Advanced Innovation Center for Genomics, College of Life Sciences, Peking University, Beijing, China.

*Corresponding author. Email: Lxyun@hebau.edu.cn

[†]These authors contributed equally to this study.

stimulus. The diameter and weight of individual uterine horns stimulated with air were recorded, and both uterine horns were graded by using a described previously scoring method.³⁴ Intravenous injection of trypan blue (T0776, Sigma, Beijing, China) dye solution was used to identify sites of increased uterine vascular permeability.⁹

Air-induced decidualization in pregnant mice. Female CD1 mice were mated with fertile males; females with vaginal plugs the following morning were considered to be at day 0.5 of pregnancy. On the afternoon of days 1.5, 2.5, 3.5, and 4.5, pregnant females underwent air infusion into a unilateral uterine horn by using TCET devices; in contralateral (control) horns, normal embryo implantation was allowed to occur. Uterine tissues were collected on day 7.5. Conceptuses were mechanically isolated from decidua by using fine forceps, and their morphologic structure was examined.

Tetraploid embryo-induced decidualization. Tetraploid embryos were prepared as described previously.¹⁹ Briefly, to induce superovulation, female mice were injected with 7.5 IU pregnant mare serum gonadotropin (Sansheng Biologic Technology, Zhejiang, China), followed 48 h later by injection of 7.5 IU human chorionic gonadotropin (Sansheng Biologic Technology, Zhejiang, China), and then were mated with males. The presence of a vaginal plug the next morning was taken as evidence of mating. On the morning of pregnancy day 1.5, female mice were killed by cervical dislocation, and the oviducts were removed and flushed with M2 medium (catalog no. M7167, Sigma) to recover the 2-cell embryos. The 2-cell embryos were placed between 2 platinum electrodes laid 1mm apart in a nonelectrolyte solution containing 0.3M mannitol (catalog no. M9546, Sigma), 0.1mM calcium chloride (catalog no. C7902, Sigma), 0.1mM magnesium sulfate (catalog no. M2643, Sigma), and 0.3% bovine serum albumin (catalog no. B2064, Sigma) in an electrode chamber (model GSS-1000, BLS, Hungary). The blastomeres were fused by 2 short electric pulses (150 V for 100 μ s) applied by using a pulse generator (model CF-150B, BLS). After 60min in culture, embryos that had not undergone fusion were discarded. The fused embryos, which were deemed tetraploid, were then cultured in KSOM medium (catalog no. MR-121-D, Millipore Sigma, Darmstadt, Germany) in an incubator (model 311, Thermo Scientific, Beijing, China). The tetraploid embryos were surgically transferred into the right oviducts of pseudopregnant day 0.5 mice. After 3 d, these mice underwent intrauterine air infusion into the left uterine horns. Uterine tissues were collected on day 7.5.

Oocyte-induced decidualization. Ovaries were isolated from female mice, put into a 35-mm dish, macerated by using scissors, and then suspended in M2 medium. Germinal vesicle (GV) oocytes were collected and transferred (12 GV oocytes per recipient) into a single uterine horn of day 3.5 pseudopregnant mice by using TCET devices. Uterine tissues were collected on day 7.5.

Embryo transfer. Naturally matured blastocysts (6 to 10; with or without air) were transferred into a single uterine horn in day 2.5 pseudopregnant mice by using TCET devices. Pregnant recipients were necropsied on day 7.5, and embryo implantation and uterine decidualization were examined. Tetraploid embryos were surgically transferred into the oviducts of day 0.5 pseudopregnant female mice, each of which received either a single 0.1-mL subcutaneous injection of flunixin (2.5 mg/kg; Unovet Pharmaceuticals, Shandong, China) immediately after anesthetic induction through intraperitoneal injection of 1.25% avertin solution (0.2 mL/10 g of body weight; catalog no. T48402, Aldrich, Beijing, China). The mice then were prepared aseptically for flank laparotomy. Briefly, a single 5-mm

incision was made in the right dorsal flank. The right oviduct was exposed. The 12 tetraploid embryos were transferred into the oviduct by using a glass transfer pipette. The oviduct was replaced carefully into the body cavity, and the skin was closed by using 1 or 2 sterile wound clips (Globalebio, Beijing, China). After 3 d, these mice again underwent intrauterine air infusion into the left uterine horn by using a glass transfer pipette. The mice were observed continuously until recovery from anesthesia and then daily until uterine tissue collection.

RNA sequencing. Three different deciduoma or decidua tissues induced by using air, tetraploid embryos, or natural embryos were collected, and conceptus tissues (embryo and trophoblast) were carefully removed from these tissues. Total RNA was extracted by using TRIzol reagent (Invitrogen, Beijing, China) from the harvested specimens. ATruSeq RNA sample preparation kit (Illumina China, Beijing) was used to generate RNA-seq libraries according to the manufacturer's protocol. High-throughput sequencing (HiSeq 2500 system, Illumina) was completed, and adaptor sequences were trimmed from raw RNA-seq data. Then reads with adaptor contaminants (length, 37bp or shorter) and low-quality sequence ($n > 10\%$) were removed for quality control. The remaining sequences were aligned to the mm10 mouse transcriptome (UCSC Genome Browser, University of California, Santa Cruz, CA) by using TopHat (version 2.0.12),^{14,36} and uniquely aligned reads were assembled by using Cufflinks and normalized as fragments per kilobase of transcript per million fragments mapped (FPKM).³⁷ FPKM values were then normalized by \log_2 (FPKM+1) for the subsequent analysis. Marker genes of each group were identified by using the Seurat find all markers function (thresh.test, 1; test.use, bimod; return.thresh, 0.01), and genes with fold-change > 1 and P value < 0.01 were selected as marker genes. Gene ontology (GO) analysis of marker genes was performed by using DAVID (<https://david.ncifcrf.gov/home.jsp>).¹⁵

Gene network analysis. The gene network was generated by using the STRING database version 10.0.³⁵ The minimum combined score was set to 0.9. Cytoscape software (www.cytoscape.org) was used for visualization and analysis of the gene network. The degree distribution was analyzed by using the Cytoscape plugin Network Analyzer.¹

Validation by quantitative real time-PCR analysis. Total RNA was extracted by using TRIzol (Invitrogen). cDNA was synthesized by using the PrimeScript reverse-transcriptase reagent kit (TaKaRa, Dalian, China). Quantitative real-time PCR analysis was performed by using the SYBR Premix Ex TaqTM kit (TaKaRa) on an IQ5 system (Bio-Rad, Shanghai, China). Glyceraldehyde 3-phosphate dehydrogenase (*Gapdh*) served as the reference gene for normalization. Primer sequences are listed in Figure 1.

Statistical analysis. Groups were compared by using paired Student t tests and one-way ANOVA in SPSS 22.0 (<https://www.ibm.com/products/spss-statistics>). A P value less than 0.05 was considered statistically significant. Results are presented as mean \pm 1 SD.

Results

Air-induced decidualization in pseudopregnant mice. To choose an appropriate volume of air for intrauterine infusion in this study, we using TCET devices to infuse 0.5, 1.0, 2.0, 5.0, or 10.0 μ L into the uterine lumen of 8 day 3.5 pseudopregnant mice. At 4 d after air infusion, all of the mice displayed a dilated and nonbeaded appearance, consistent with decidualization, in the infused uterine horn (Figure 2 A). This phenomenon did not occur in the contralateral uterine horn, indicating that

Gene	Forward sequence	Reverse sequence	Amplicon (bp)
<i>H19</i>	GAAATGGTGCTACCCAGTCAT	TTCAGCTTCACCTTGGAGCAG	140
<i>Prl5a1</i>	ATGGCTGATCTCGATGGAAC	TGACCAGGCAGGGTAGTCTT	158
<i>Mmp9</i>	AACACCACCGAGCTATCCAC	AGGAGTCTGGGGTCTGGTTT	163
<i>Cts7</i>	GCCTTCATAGCCATAGCCAA	CCTTTCATTCATATCGGGGA	98
<i>Mmp1a</i>	GCTCAGGTTCTGGCATGAAT	AACAGGTGCAACAACACCAC	134
<i>Prl2c3</i>	GACACATTTGAATTAGCCGG	AGAAGAGCTGCATAGTGTG	194
<i>Prl4a1</i>	GTGGAATCAGGCAATCCAGT	TGGATCTTTGGGCTTGTTT	171
<i>Prl7a1</i>	CGCTGTCTTCACTCAACCA	CATGGCATGATCCAACAGTC	152
<i>Gapdh</i>	TGCTGCTTACCACCTTC	GCCTCCGTGTTCTACCC	93

Figure 1. Primers and amplicon length of evaluated genes.

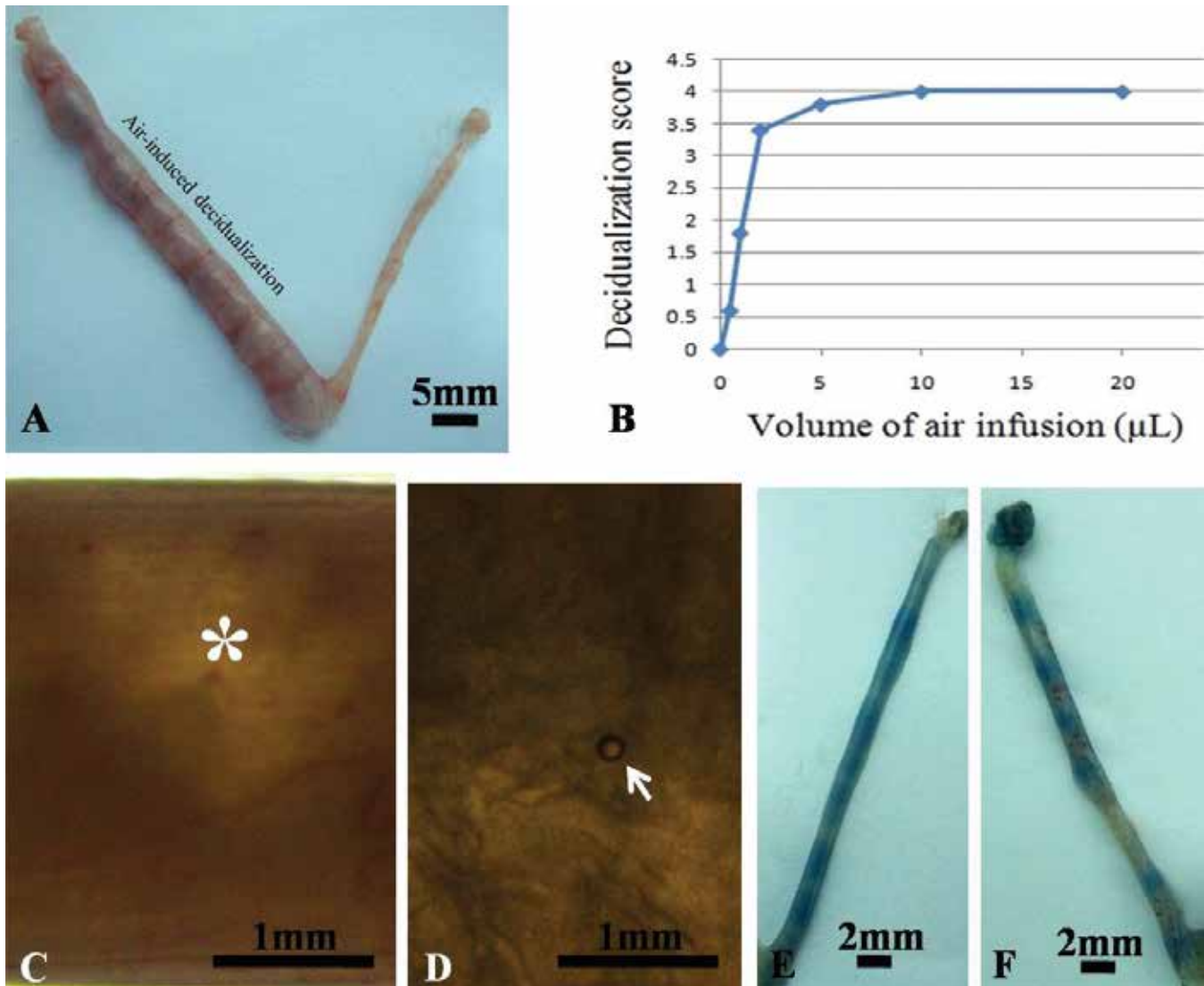


Figure 2. Intrauterine air-induced decidualization. (A) Air (2.0 µL) was infused into a single uterine horn of a pseudopregnant day 3.5 mouse. After 4 d, the right horn showed decidualization. (B) Relationship between the volume of intrauterine air infusion and decidualization. (C) A large intrauterine air bubble (asterisk) was observed immediately after air infusion into uterine horns. (D) Microbubbles (arrowhead) were detected at 2 h after air infusion. (E) Air was infused into a single uterine horn of a pseudopregnant day 3.5 mouse. After 1 d, the mouse was anesthetized and the tail veins injected with 0.1 mL of 1% trypan blue in saline. The unilateral uterine horn contained a diffuse blue area. (F) A natural day 4.5 pregnant uterine horn displayed distinct and isolated blue bands after the trypan blue injection.

decidualization was induced by the infused air. The mean weight of the uterine horns infused with air (725 ± 170 mg) was significantly ($P < 0.001$) greater than noninfused horns (74 ± 37 mg, $n = 8$); the mean diameter of air-infused horns was greater ($P < 0.001$) as well (5.8 ± 1.2 mm compared with 1.3 ± 0.7 mm, $n = 8$). Decidualization induced by different volumes of infused air yielded different scores. At volumes of 2.0 µL and lower, the score was positively correlated ($r = 0.99$, $P < 0.001$)

with the volume of air infused; at volumes above 2.0 µL, the score did not increase with the increase in air volume. In light of these data, we selected a dose of 2.0 µL of air for all subsequent experiments (Figure 2 B). Decidualization did not occur when air was infused into a single uterine lumen of day 2.5 ($n = 6$) or day 1.5 ($n = 6$) pseudopregnant mice.

We euthanized 3 day 3.5 pseudopregnant mice immediately after air infusion and isolated the uterine tissues. Stereomicroscopy

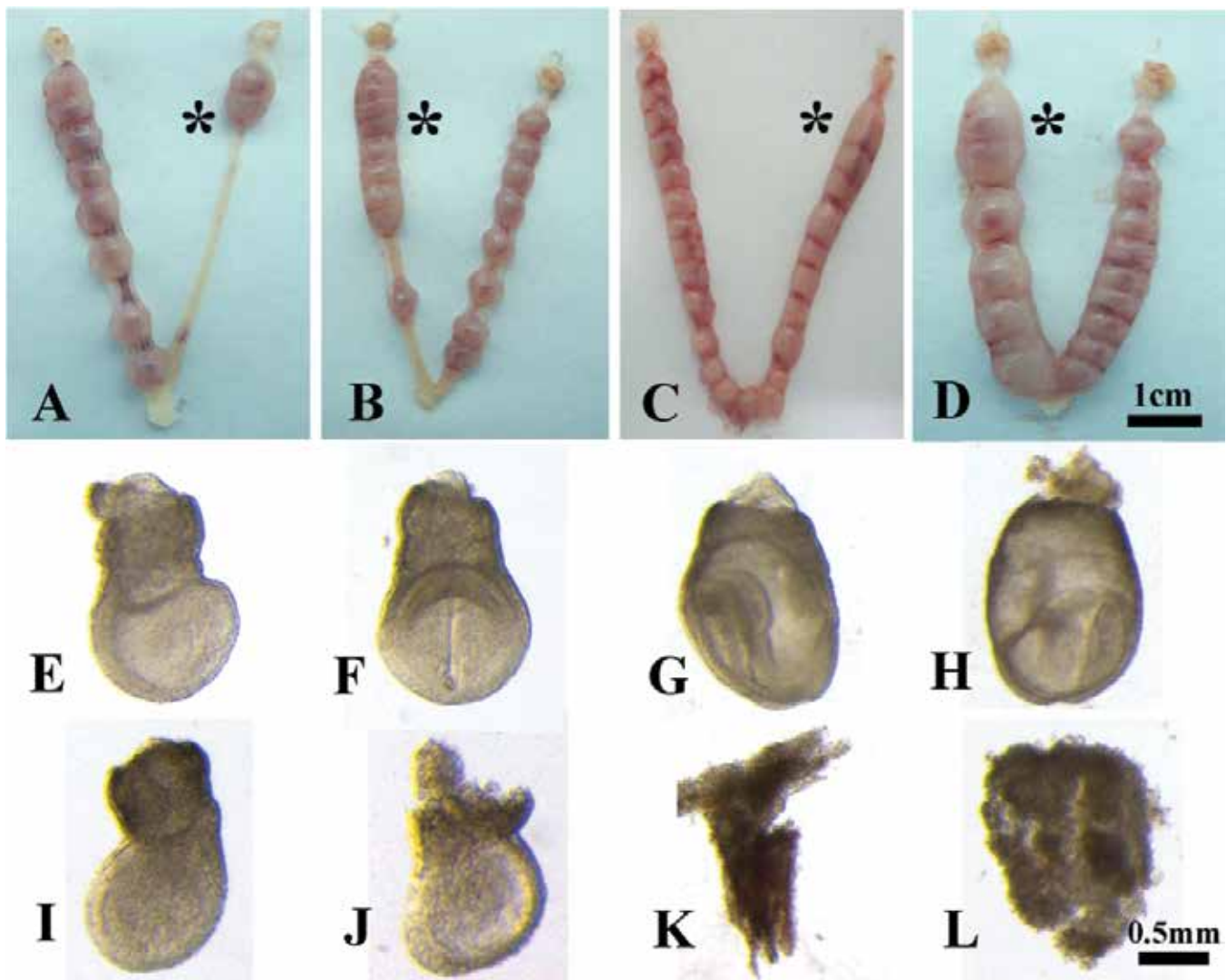


Figure 3. Intrauterine air disrupted postimplantation embryonic development. Air were infused into a single uterine horn (asterisk) of pregnant mice. (A) Day 1.5. (B) Day 2.5. (C) Day 3.5. (D) Day 4.5. The contralateral uterine horn without air infusion was used as a control. On day 7.5, fetal development was significantly superior in the (E through H) control horns than in the (I through L) air-infused horns.

revealed uterine lumens that were filled with large bubbles (Figure 2 C). In addition, the uterine horns of 3 day 3.5 pseudopregnant mice killed at 2h after air infusion contained micro air bubbles in the uterine lumens (Figure 2 D).

We further examined whether intrauterine air bubbles increased endometrial capillary permeability. To this end, we used TCET devices to infuse air into a single uterine lumen in each of 3 day 3.5 pseudopregnant mice. After 1 d, the mice were anesthetized intraperitoneally by using avertin, and the tail veins were injected with 0.1 mL of 1% trypan blue in saline. After 3 min, the air-infused uterine horns of the 3 mice displayed a diffuse blue area (Figure 2 E). In contrast, the natural day 4.5 pregnant horn displayed distinct and isolated blue bands after trypan blue injection (Figure 2 F).

Effects of intrauterine air infusion on fetal development in naturally pregnant mice. Air (2.0 μ L) was infused into a single uterine lumen ($n = 12$) of day 1.5, 2.5, 3.5, and 4.5 pregnant mice. On day 7.5, the uterine tissues of 4 females in each group were collected; the number of live pups and birth weight were recorded at delivery in the remaining dams.

Among all 4 groups, all 48 mice with vaginal plugs became pregnant; 32 of them had pups. The number and birthweight of

live pups (mean \pm 1 SD) for each group were 9.3 ± 1.5 and 1.38 ± 0.14 g, 9.0 ± 1.7 and 1.4 ± 0.12 g, 6.1 ± 1.9 and 1.42 ± 0.13 g, and 6.3 ± 2.1 and 1.35 ± 0.18 g, respectively. Dams infused when 3.5 or 4.5 d pregnant had fewer ($P < 0.01$) live pups than those infused on day 1.5 or 2.5, but birth weight did not differ significantly among the 4 groups. The left and right uterine horns of the 16 day 7.5 females displayed visible morphologic differences (Figure 3 A through D). In mice infused on day 1.5 or 2.5 of pregnancy, the conceptuses in the air-infused horns were crowded around and unevenly distributed along the uterine lumens compared with the noninfused horns (Figure 3 A and B). In dams infused on day 3.5 or 4.5, the air-infused horns displayed similar decidualization (Figure 3 C and D), comprising a dilated and nonbeaded appearance, as the air-induced decidualization of pseudopregnant mice (Figure 2 A). In addition, in all groups, the conceptuses from noninfused horns were larger and had distinct anatomic structures (Figure 3 E through H) compared with conceptuses from air-infused horns (Figure 3 I through L). The conceptuses from the air-infused horns of dams infused on day 3.5 or 4.5 (Figure 3 K and L) had lost all anatomic structure, indicating that they were dead.

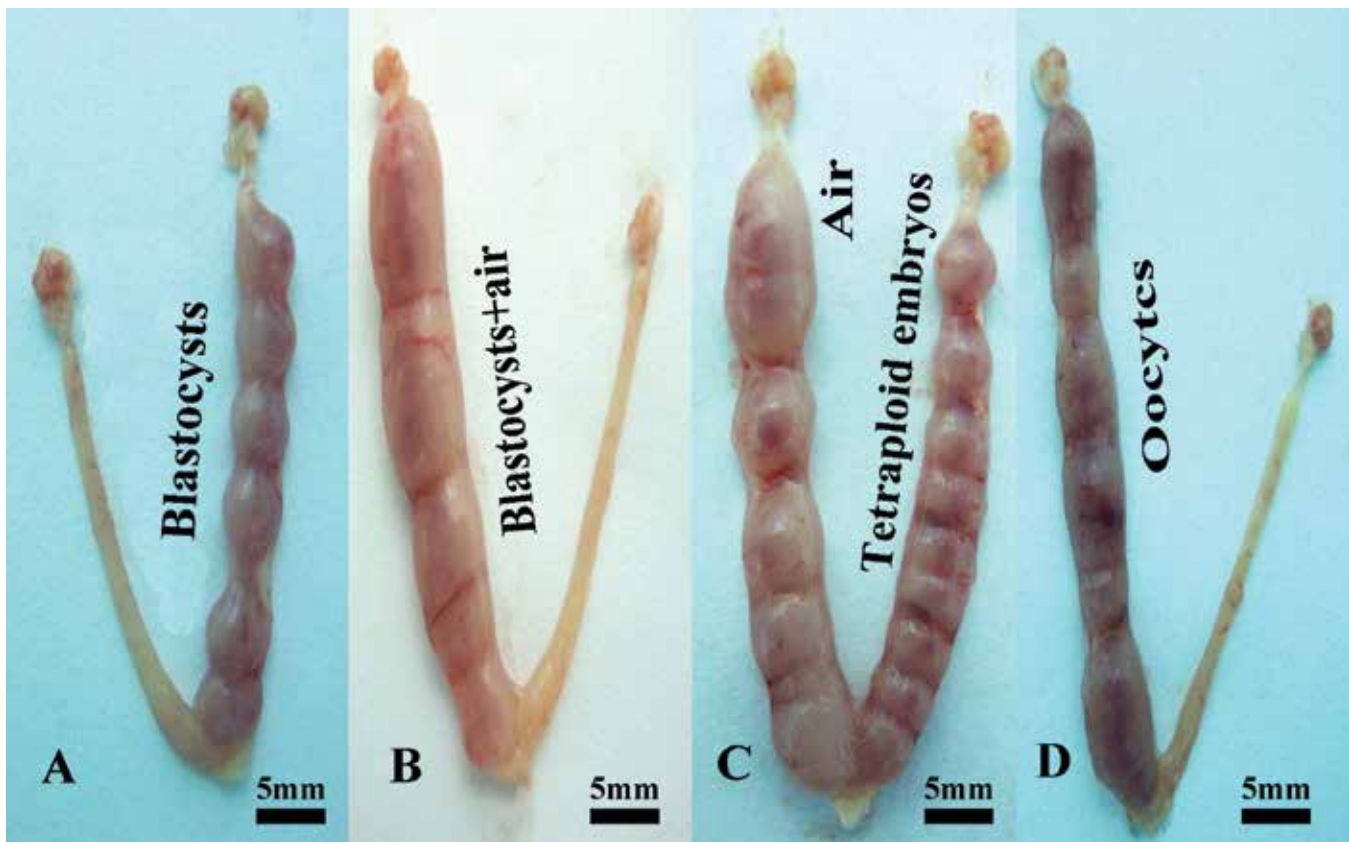


Figure 4. Decidualization on day 7.5 induced by different decidual stimuli. (A) Natural day 3.5 blastocysts were transferred into a single uterine horn of a pseudopregnant day 2.5 mouse. (B) Natural day 3.5 blastocysts and 2.0 μ L of air were transferred into a single uterine horn of a pseudopregnant day 2.5 mouse. (C) Tetraploid embryos were surgically transferred into the right oviduct of a pseudopregnant day 0.5 mouse, followed 72 h later by surgical infusion of 2.0 μ L of air into the left uterine horn. (D) Germinal vesicle oocytes were transferred into a single uterine horn of a pseudopregnant day 2.5 mouse.

Intrauterine air infusion disrupt development of transferred embryos. Blastocysts with air (2.0 μ L; $n = 48$) and 32 blastocysts without air were nonsurgically transferred unilaterally into day 2.5 pseudopregnant mice ($n = 6$ and 4, respectively). On day 7.5, 10 mice from each group were killed and uterine decidualization and conceptuses were evaluated. In the nonair group, the unilateral uterine horns of all 4 mice displayed even embryo distribution (total, 24 implantation sites) with a beaded appearance, and the conceptuses in each decidia displayed normal embryonic structure (Figure 4 A). By contrast, in the air group, all 6 mice displayed uneven decidualization, with the air-infused uterine horn showing a dilated and nonbeaded appearance and containing growth-delayed or dead conceptuses (Figure 4 B).

Oocyte- and tetraploid embryo-induced decidualization. To explore a potential underlying mechanism for the disruption of embryonic development due to air infusion, we used tetraploid embryo- (tetraploid-induced) and GV oocyte-induced (oocyte-induced) decidualization. To this end, forty-five 2-cell embryos from 4 day 1.5 pregnant mice underwent electrofusion. The fused embryos were surgically transferred into the right oviducts of 3 day 0.5 pseudopregnant mice. On day 3.5, air was surgically infused into the left uterine horns of the 3 recipients. On day 7.5, the left uterine horns of all 3 mice displayed dilated and nonbeaded decidualization, whereas the right uterine horns displayed normal and beaded implantation sites (Figure 4 C); a total of 37 implantation sites were identified. In addition, 36 GV oocytes were nonsurgically transferred into single uterine horns of 3 day 3.5 pseudopregnant mice. On day 7.5, the 3 mice

displayed decidualization with dilated and nonbeaded appearance (Figure 4 D). The oocyte-induced decidual responses were morphologically the same as those after air induction, whereas tetraploid-induced decidual responses were the same as those for embryo induction.

Genes differentially expressed among air-induced and tetraploid-induced deciduoma and embryo-induced decidua. To explore the potential effect of the air on uterine gene expression during decidualization, we compared the global mRNA levels among RNA samples from day 7.5 air-induced and tetraploid-induced deciduoma and embryo-induced decidua.

Thirty-three genes were upregulated in the embryo-induced decidua compared with the air- and tetraploid-induced deciduoma. No gene differed significantly in expression between air- and tetraploid-induced deciduoma (Figure 5). To validate the RNA sequencing data, a total of 8 genes with various fold changes (*H19*, *Prl5a1*, *Mmp9*, *Cts7*, *Mmp1a*, *Prl2c3*, *Prl4a1*, and *Prl7a1*) were selected and validated by quantitative real time-PCR analysis (Table 1). Although the fold change varied between PCR and RNA-seq data, the overall expression patterns were coincident between these 2 techniques, indicating the high quality of our RNA-seq data (Table 2).

GO enrichment of differentially expressed genes. Regarding upregulated genes, 16 GO terms were significantly enriched in the biologic process category (Figure 6 A). In the molecular function category, transcripts associated with hormone activity were enriched. The over-represented GO terms under the cellular component category were representative of the extracellular region and extracellular space. In contrast, none

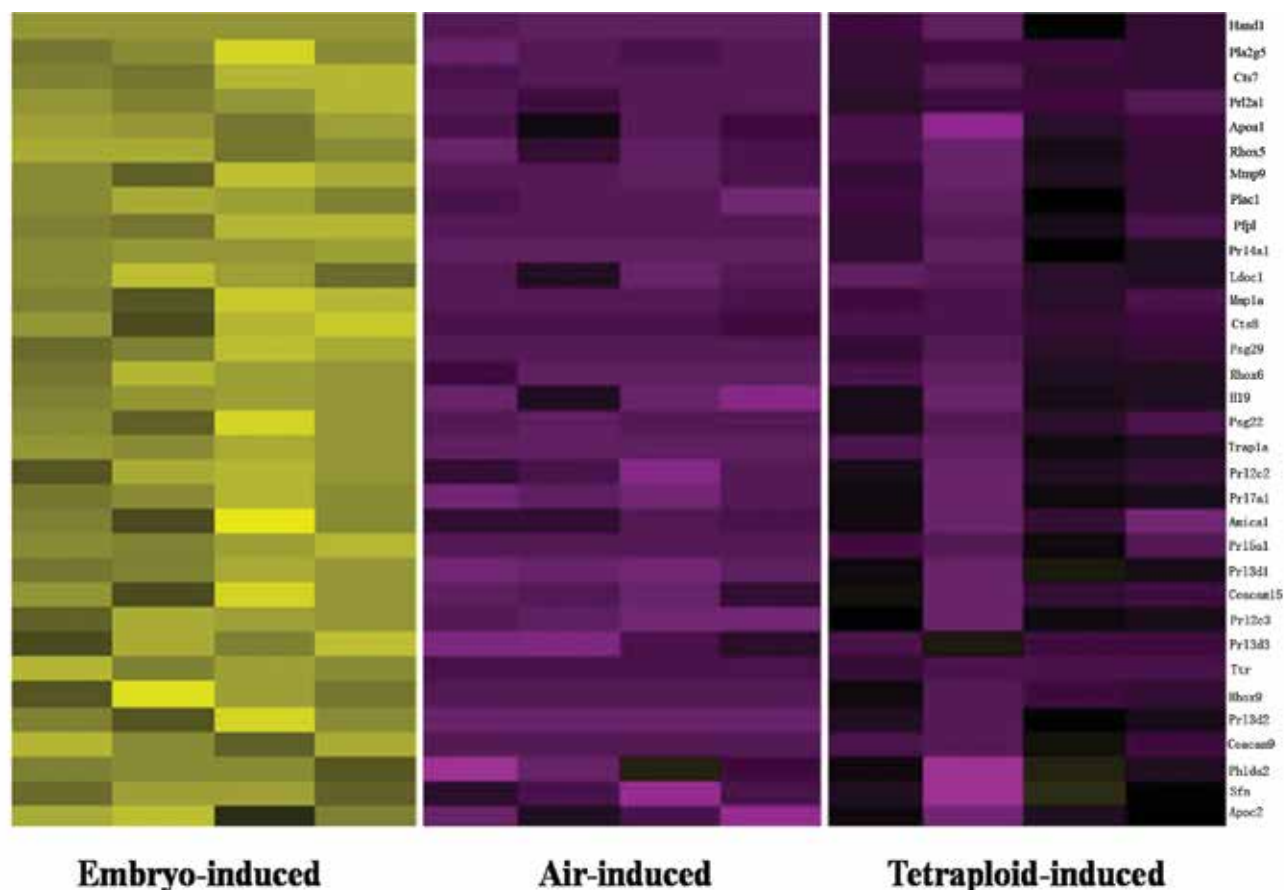


Figure 5. Heatmap of genes differentially expressed between day 7.5 embryo-induced decidua compared with air- or tetraploid-induced decidua. Yellow to black indicates a gradient of high to low expression. A total of 33 genes were upregulated in the embryo-induced decidua compared with the air- and tetraploid-induced decidua. No genes showed significant differences in expression between air- and tetraploid-induced decidua.

Table 1. Number of fragments per kilobase of transcript per million fragments mapped through RNA sequencing

Gene	Embryo-induced decidua	Air-induced deciduoma	Tetraploid-induced deciduoma
<i>H19</i>	92.6 ± 15.8	5.0 ± 3.7	10.4 ± 3.8
<i>Prl5a1</i>	16.5 ± 4.9	0.0 ± 0.0	0.4 ± 0.7
<i>Mmp9</i>	25.7 ± 11.0	0.4 ± 0.1	0.9 ± 0.6
<i>Cts7</i>	27.0 ± 11.8	0.1 ± 0.1	0.4 ± 0.2
<i>Mmp1a</i>	11.4 ± 5.9	0.0 ± 0.1	0.3 ± 0.2
<i>Prl2c3</i>	57.9 ± 23.3	0.3 ± 0.3	3.4 ± 2.4
<i>Prl4a1</i>	28.8 ± 3.1	0.0 ± 0.0	1.4 ± 1.4
<i>Prl7a1</i>	54.0 ± 20.6	0.2 ± 0.2	2.7 ± 1.7
<i>Gapdh</i>	1193 ± 77	1133 ± 219	1227 ± 175

Data are given as mean ± 1 SD.

of these GO terms in these 3 categories were enriched among downregulated genes.

Identification of gene interaction through network analysis.

We performed gene network analysis by using integrative gene interaction data from the STRING database. The gene network for 18 upregulated genes (Figure 6 B) contained 8 prolactin-related genes, the trophoblast giant cell (TGC) differentiation-promoting bHLH transcription factor *Hand1*, TGC-specific marker *Prl3d1*, 2 placenta-specific cathepsins (*Cts7*, *Cts8*), the primitive visceral endodermal markers (*Rhox5*, *Rhox6*, *Rhox9*), transthyretin (*Ttr*), and lipid transport markers (*Apoa1*, *Apoc2*).

Discussion

This study provided strong evidence that intrauterine air disrupts embryo spacing, induces deciduoma, and impairs postimplantation embryonic development. The gene expression profile of air-induced deciduoma was significantly different from that of natural embryo-induced decidua but similar to tetraploid-induced deciduoma. The data indicated that intrauterine infusion of air into the uterine horns of pregnant mice probably disrupts the process of embryo-induced decidualization. Infused air was split into numerous micro air bubbles due to uterine contraction (Figure 2 C and D). These microbubbles probably adhered to embryos and endometria and then stimulated abnormal decidualization. The resulting

Table 2. Relative gene expression according to real-time PCR analysis

Gene	Embryo-induced decidua	Air-induced deciduoma	Tetraploid-induced deciduoma
<i>H19</i>	8.9E-04 ± 2.6E-04	6.1E-05 ± 1.6E-05	1.5E-04 ± 9.5E-05
<i>Prl5a1</i>	3.6E-03 ± 2.0E-03	9.5E-07 ± 7.2E-07	6.0E-04 ± 7.6E-04
<i>Mmp9</i>	2.9E-03 ± 1.3E-03	7.0E-05 ± 2.3E-05	5.9E-04 ± 5.6E-04
<i>Cts7</i>	5.1E-03 ± 2.4E-03	1.3E-06 ± 2.4E-06	8.1E-04 ± 1.2E-03
<i>Mmp1a</i>	1.3E-03 ± 7.0E-04	4.8E-07 ± 2.8E-07	1.4E-04 ± 1.4E-04
<i>Prl2c3</i>	7.9E-03 ± 4.5E-03	3.7E-05 ± 1.7E-05	1.9E-03 ± 1.8E-03
<i>Prl4a1</i>	6.2E-03 ± 2.9E-03	4.5E-07 ± 5.3E-08	1.3E-03 ± 1.9E-03
<i>Prl7a1</i>	2.9E-03 ± 8.9E-04	3.4E-06 ± 1.7E-06	7.5E-04 ± 6.6E-04

Data (no. copies of target gene / no. of copies of *Gapdh*) are given as mean ± 1 SD.

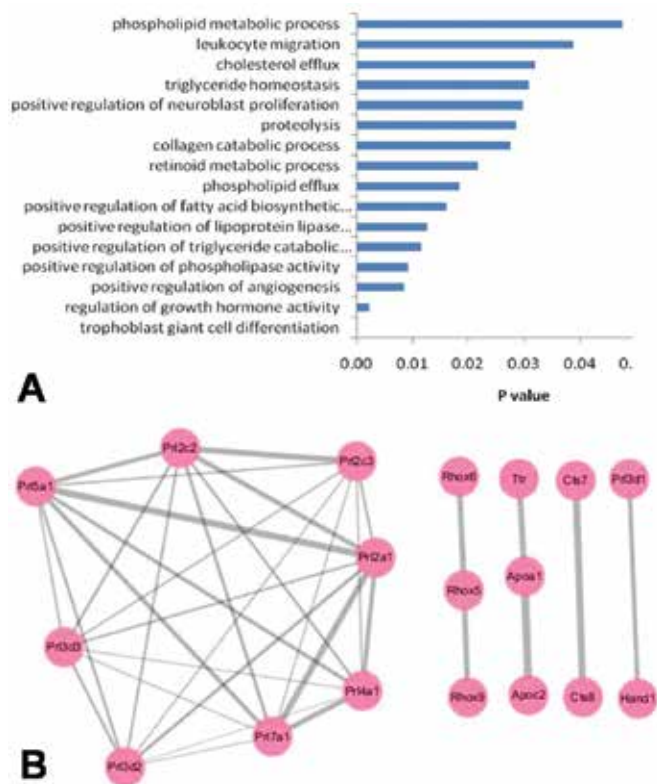


Figure 6. (A) Gene ontology enrichment chart of upregulated genes in biologic process category and (B) the protein interaction network of genes highly expressed in embryo-induced decidua.

tissues resembled deciduoma rather than decidua in morphology and gene expression profiling. Although only select species are said to exhibit uterine decidualization, similar changes have been suggested to occur in other species including those where implantation is superficial,^{16,17,22} therefore intrauterine air likely disrupts embryonic development in these species. Although less than 1.0 μ L of air typically is transferred with embryos into murine uterine horns,²⁶ trace air potentially may significantly disrupt embryonic development, and these data suggested that air should be excluded from the catheter during murine embryo transfer. Oviduct transfer in day 0.5 recipients or blastocyst transfer in day 2.5 recipients is used in many facilities internationally. In pilot experiments for the current study, air and embryos that were cotransferred into oviducts did not disrupt decidualization and embryonic development. Although air can impair embryonic development after blastocyst transfer into both day 2.5 and 3.5 recipients, the impairment was more severe in day 3.5 recipients.

Infused air did not induce deciduoma in day 1.5 and 2.5 pregnant mice. The likely reason is that the air bubbles have disappeared from the uterine lumens by the time the window of receptivity occurs on day 3.5. The air bubbles probably were expelled from uterine lumens through uterine contraction or were resorbed.^{4,23} However, the air bubbles disrupted embryo spacing along the longitudinal axis, such that all of the embryos became crowded together near the uterus-oviduct junction. This distribution may have resulted because uterine peristalsis led to intrauterine air bubble movement, subsequently pushing the embryos together. Although air did not induce deciduoma in day 2.5 pseudopregnant mice, it did induce decidualization in day 2.5 pseudopregnant mice after blastocyst transfer, indicating that blastocysts stimulate the appearance of a window of receptivity.^{20,21}

Artificially induced deciduoma due to a nonphysiologic decidogenic stimulus (oil, bead, air, oocytes) usually displays an even sausage-like or uneven bead appearance.^{8,11} These morphologic differences probably depends on the magnitude of stimulus rather than any intrinsic quality of stimulus. That is, deciduoma displays an even sausage-like appearance when numerous stimulus sites are present. In contrast, deciduoma has an uneven bead appearance when only a few stimulus sites occur. In many previous studies, oil-induced deciduoma usually displayed a sausage-like appearance.¹⁰ After intrauterine infusion, oil likely was split into numerous micro drops due to uterine contraction,^{4,23} and the drops moved randomly and distributed throughout the entire uterine lumen. This distribution might lead to the development of numerous deciduogenic stimulus sites and sausage-like deciduoma. Intrauterine-infused air might similarly be split into many micro air bubbles.⁶ In the current study, air-induced deciduoma usually displayed a sausage-like appearance when more than 2 μ L of air was infused. Indeed, the diffuse blue area in Figure 1 E indicated a large number of stimulus sites and a sausage-like appearance. However, in pilot studies, when infused air was less than 1 μ L, the deciduoma usually displayed uneven beads (data not shown). Air- and oocyte-induced decidual responses were similar in morphology, whereas tetraploid- and embryo-induced decidual responses resembled each other morphologically, and tetraploid induction was completely indistinguishable from pregnant decidualization in morphology. This tetraploid model of decidualization likely is more 'physiologic' than other artificial methods of inducing decidualization, including concanavalin A-coated Sepharose beads.^{13,24,33} However, gene expression profiling in tetraploid-induced decidualization differed significantly different from naturally pregnant decidualization. Consequently, the tissues resulting from tetraploid induction technically are deciduoma instead of decidua.

The present study exploited the decidual activity of GV oocytes in pseudopregnant mice. The introduction of 12 GV oocytes into the lumen of a uterine horn of a day 3.5 pseudo-pregnant mouse induced a decidual response that was virtually indistinguishable in morphology from that produced by using concanavalin A-coated Sepharose beads.^{13,24,33} Therefore GV oocyte-induced deciduoma provides a simple and inexpensive model of focal decidual stimulus and localized decidualization.

In this study, we assessed a subset of 33 genes whose expression in the uterus during decidualization may be regulated by molecular signals from ICM (Figure 5). However, these genes showed decreased expression in embryo-induced decidua (Table 2). In this study, all of the decidual tissues were collected on day 7.5 of pregnancy, at the initiation of decidual regression.³² According to GO analysis, the 33 differentially expressed genes likely participated in decidualization by regulating TGC differentiation (Figure 6 A). TGC participate in several processes essential to successful pregnancy, including blastocyst implantation, remodeling of maternal decidua, and secretion of hormones that regulate the development of both the fetal and maternal compartments of the placenta.²⁵

The mouse preimplantation blastocyst consists of 2 cell types, the trophectoderm and ICM. The trophectoderm is a functional epithelium that is responsible for initiating decidualization, mediating attachment with and implantation into the uterine wall, and subsequently contributing to the placenta, whereas the ICM gives rise to all cell types of the embryo proper as well as some nontrophoblastic extraembryonic tissues.^{3,30} Tetraploid blastocysts have a functional trophectoderm but lack a functional ICM.²⁹ As such, tetraploid blastocysts are not independently capable of completing normal development but, when complemented by the introduction of ICM cells, they develop into mature fetuses in which embryonic lineages are derived entirely from the ICM cells, and extraembryonic lineages arise largely from the tetraploid component. This approach is often referred to as tetraploid complementation.²⁷ Tetraploid-induced deciduoma was morphologically indistinguishable from natural embryo-induced decidua: all of them displayed an even bead appearance and regular distribution along the uterine longitudinal axis. However, the gene expression profile of tetraploid-induced deciduoma was significantly different from that of natural embryo-induced decidua and was almost identical to that of air-induced deciduoma.

Our data suggest that whereas the morphologic differences among tetraploid-, air-, and embryo-induced deciduoma and decidua may depend on the trophectoderm, the difference in gene expression may depend on the ICM. Because of the lack of a functional ICM, tetraploid-induced deciduoma displayed a similar gene expression profile to that of air-induced deciduoma. We therefore propose that the ICM plays a key role in regulating decidualization.

Given our current results, the traditional view of an antagonistic relationship between the conceptus and the uterus should be revised;² instead, an ICM-directed decidualization model is perhaps more appropriate. A relay mechanism exists among the ICM, trophectoderm, uterine endometria, and other target cells. As an intermediate, the trophectoderm relays ICM-derived signals to other target cells. If the ICM is not developing well, the trophectoderm relays 'no/wrong' signals regarding decidualization, and pregnancy failure would result. This ICM-directed decidualization model was suggested previously, prior to previous conceptus-directed decidualization model.^{2,18,38} In addition, the roles of the ICM-directed changes in gene expression are

likely related to TGC differentiation and placental development (Figure 5 A). The discovery of genes whose expression in the decidua are dependent on the presence of a functional ICM has very important clinical implications. This association may provide an innovative approach to detect the developmental status of embryos in human reproductive medicine.

Acknowledgments

We thank Professor Derrick Rancourt (Departments of Oncology, Chemistry and Molecular Biology, and Medical Genetics at the University of Calgary) for his critical remarks and for editing this manuscript. This work was supported by the National Key R&D Program of China (2017YFD0501901).

References

1. Assenov Y, Ramírez F, Schelhorn SE, Lengauer T, Albrecht M. 2007. Computing topological parameters of biological networks. *Bioinformatics* **24**:282–284. <https://doi.org/10.1093/bioinformatics/btm554>.
2. Bany BM, Cross JC. 2006. Post-implantation mouse conceptuses produce paracrine signals that regulate the uterine endometrium undergoing decidualization. *Dev Biol* **294**:445–456. <https://doi.org/10.1016/j.ydbio.2006.03.006>.
3. Bedzhov I, Graham SJ, Leung CY, Zernicka-Goetz M. 2014. Developmental plasticity, cell fate specification, and morphogenesis in the early mouse embryo. *Philos Trans R Soc Lond B Biol Sci* **369**:1–14. <https://doi.org/10.1098/rstb.2013.0538>. Correction: 2015. *Philos Trans R Soc Lond B Biol Sci* <https://doi.org/10.1098/rstb.2014.0339>.
4. Chen Q, Zhang Y, Elad D, Jaffa AJ, Cao Y, Ye X, Duan E. 2013. Navigating the site for embryo implantation: biomechanical and molecular regulation of intrauterine embryo distribution. *Mol Aspects Med* **34**:1024–1042. <https://doi.org/10.1016/j.mam.2012.07.017>. Erratum: 2013. *Mol Aspects Med* **34**:1257.
5. Christianson MS, Zhao Y, Shoham G, Granot I, Safran A, Khafagy A, Leong M, Shoham Z. 2014. Embryo catheter loading and embryo culture techniques: results of a worldwide Web-based survey. *J Assist Reprod Genet* **31**:1029–1036. <https://doi.org/10.1007/s10815-014-0250-z>.
6. Confino E, Zhang J, Risquez F. 2007. Air bubble migration is a random event post embryo transfer. *J Assist Reprod Genet* **24**:223–226. <https://doi.org/10.1007/s10815-007-9120-2>.
7. Cui L, Zhang Z, Sun F, Duan X, Wang M, Di K, Li X. 2014. Transcervical embryo transfer in mice. *J Am Assoc Lab Anim Sci* **53**:228–231.
8. Dearden-Badet MT. 1986. Comparative study of biological properties of proteins synthesised in vitro by murine decidua and deciduoma. *Am J Reprod Immunol Microbiol* **10**:20–25. <https://doi.org/10.1111/j.1600-0897.1986.tb00004.x>.
9. Deb K, Reese J, Paria BC. 2006. Methodologies to study implantation in mice. *Methods Mol Med* **121**:9–34.
10. Ezoe K, Daikoku T, Yabuuchi A, Murata N, Kawano H, Abe T, Okuno T, Kobayashi T, Kato K. 2014. Ovarian stimulation using human chorionic gonadotrophin impairs blastocyst implantation and decidualization by altering ovarian hormone levels and downstream signaling in mice. *Mol Hum Reprod* **20**:1101–1116. <https://doi.org/10.1093/molehr/gau065>.
11. Grant PS, McLaren A. 1973. Egg implantation and deciduoma induction in cyclic mice after treatment with progestagens and oestradiol. *J Reprod Fertil* **34**:415–421. <https://doi.org/10.1530/jrf.0.0340415>.
12. Herington JL, Bany BM. 2009. Do molecular signals from the conceptus influence endometrium decidualization in rodents? *J Exp Zool B Mol Dev Evol* **312**:797–816. <https://doi.org/10.1002/jez.b.21308>.
13. Herington JL, Underwood T, McConaha M, Bany BM. 2009. Paracrine signals from the mouse conceptus are not required for the normal progression of decidualization. *Endocrinology* **150**:4404–4413. <https://doi.org/10.1210/en.2009-0036>.

14. Hinrichs AS, Karolchik D, Baertsch R, Barber GP, Bejerano G, Clawson H, Diekhans M, Furey TS, Harte RA, Hsu F, Hillman Jackson J, Kuhn RM, Pedersen JS, Pohl A, Raney BJ, Rosenbloom KR, Siepel A, Smith KE, Sugnet CW, Sultan Qurraie A, Thomas DJ, Trumbower H, Weber RJ, Weirauch M, Zweig AS, Haussler D, Kent WJ. 2006. The UCSC genome browser database: update 2006. *Nucleic Acids Res* **34**:D590–D598. <https://doi.org/10.1093/nar/gkj144>.
15. Huang Da W, Sherman BT, Lempicki RA. 2009. Systematic and integrative analysis of large gene lists using DAVID bioinformatics resources. *Nat Protoc* **4**:44–57. <https://doi.org/10.1038/nprot.2008.211>.
16. Johnson GA, Burghardt RC, Joyce MM, Spencer TE, Bazer FW, Pfarrer C, Gray CA. 2003. Osteopontin expression in uterine stroma indicates a decidualization-like differentiation during ovine pregnancy. *Biol Reprod* **68**:1951–1958. <https://doi.org/10.1095/biolreprod.102.012948>.
17. Joyce MM, Gonzalez JF, Lewis S, Woldesenbet S, Burghardt RC, Newton GR, Johnson GA. 2005. Caprine uterine and placental osteopontin expression is distinct among epitheliochorial implanting species. *Placenta* **26**:160–170. <https://doi.org/10.1016/j.placenta.2004.05.009>.
18. Kashiwagi A, DiGirolamo CM, Kanda Y, Niikura Y, Esmon CT, Hansen TR, Shioda T, Pru JK. 2007. The postimplantation embryo differentially regulates endometrial gene expression and decidualization. *Endocrinology* **148**:4173–4184. <https://doi.org/10.1210/en.2007-0268>.
19. Kaufman MH, Webb S. 1990. Postimplantation development of tetraploid mouse embryos produced by electrofusion. *Development* **110**:1121–1132.
20. Li S, Wang TS, Qin FN, Huang Z, Liang XH, Gao F, Song Z, Yang ZM. 2015. Differential regulation of receptivity in 2 uterine horns of a recipient mouse following asynchronous embryo transfer. *Sci Rep* **5**:15897. <https://doi.org/10.1038/srep15897>.
21. López-Cardona AP, Fernández-González R, Pérez-Crespo M, Alén F, de Fonseca FR, Orío L, Gutiérrez-Adán A. 2015. Effects of synchronous and asynchronous embryo transfer on postnatal development, adult health, and behavior in mice. *Biol Reprod* **93**:1–6. <https://doi.org/10.1095/biolreprod.115.130385>.
22. MacIntyre DM, Lim HC, Ryan K, Kimmins S, Small JA, MacLaren LA. 2002. Implantation-associated changes in bovine uterine expression of integrins and extracellular matrix. *Biol Reprod* **66**:1430–1436. <https://doi.org/10.1095/biolreprod66.5.1430>.
23. Martin L. 1979. Early cellular changes and circular muscle contraction associated with the induction of decidualization by intrauterine oil in mice. *J Reprod Fertil* **55**:135–139. <https://doi.org/10.1530/jrf.0.0550135>.
24. McConaha ME, Eckstrum K, An J, Steinle JJ, Bany BM. 2011. Microarray assessment of the influence of the conceptus on gene expression in the mouse uterus during decidualization. *Reproduction* **141**:511–527. <https://doi.org/10.1530/REP-10-0358>.
25. Nadra K, Anghel SI, Joye E, Tan NS, Basu-Modak S, Trono D, Wahl W, Desvergne B. 2006. Differentiation of trophoblast giant cells and their metabolic functions are dependent on peroxisome proliferator-activated receptor β/δ . *Mol Cell Biol* **26**:3266–3281. <https://doi.org/10.1128/MCB.26.8.3266-3281.2006>.
26. Nagy A, Gertsenstein M, Vintersten K, Behringer R. 2003. Manipulating the mouse embryo: a laboratory manual, 3rd ed. p 268–271. New York (NY): Cold Spring Harbor Press.
27. Nagy A, Góczy E, Diaz EM, Prideaux VR, Iványi E, Markkula M, Rossant J. 1990. Embryonic stem cells alone are able to support fetal development in the mouse. *Development* **110**:815–821.
28. Orsini MW. 1963. Induction of decidualomata in hamster and rat by injected air. *J Endocrinol* **28**:119–121. <https://doi.org/10.1677/joe.0.0280119>.
29. Park MR, Hwang KC, Bui HT, Cho SG, Park C, Song H, Oh JW, Kim JH. 2012. Altered gene expression profiles in mouse tetraploid blastocysts. *J Reprod Dev* **58**:344–352. <https://doi.org/10.1262/jrd.11-110M>.
30. Pfeffer PL, Pearton DJ. 2012. Trophoblast development. *Reproduction* **143**:231–246. <https://doi.org/10.1530/REP-11-0374>.
31. Phillips PE, Jahnke MM. 2016. Embryo transfer (techniques, donors, and recipients). *Vet Clin North Am Food Anim Pract* **32**:365–385. <https://doi.org/10.1016/j.cvfa.2016.01.008>.
32. Ramathal CY, Bagchi IC, Taylor RN, Bagchi MK. 2010. Endometrial decidualization: of mice and men. *Semin Reprod Med* **28**:17–26. <https://doi.org/10.1055/s-0029-1242989>.
33. Sakoff JA, Murdoch RN. 1994. Alterations in uterine calcium ions during induction of the decidual cell reaction in pseudopregnant mice. *J Reprod Fertil* **101**:97–102. <https://doi.org/10.1530/jrf.0.1010097>.
34. Shelesnyak MC, Kraicer PF. 1961. A physiological method for inducing experimental decidualization of the rat uterus: standardization and evaluation. *J Reprod Fertil* **2**:438–446. <https://doi.org/10.1530/jrf.0.0020438>.
35. Szklarczyk D, Franceschini A, Wyder S, Forslund K, Heller D, Huerta-Cepas J, Simonovic M, Roth A, Santos A, Tsafou KP, Kuhn M, Bork P, Jensen LJ, von Mering C. 2014. STRING v10: protein–protein interaction networks, integrated over the tree of life. *Nucleic Acids Res* **43**:D447–D452. <https://doi.org/10.1093/nar/gku1003>.
36. Trapnell C, Pachter L, Salzberg SL. 2009. TopHat: discovering splice junctions with RNA-Seq. *Bioinformatics* **25**:1105–1111. <https://doi.org/10.1093/bioinformatics/btp120>.
37. Trapnell C, Williams BA, Pertea G, Mortazavi A, Kwan G, van Baren MJ, Salzberg SL, Wold BJ, Pachter L. 2010. Transcript assembly and quantification by RNA-Seq reveals unannotated transcripts and isoform switching during cell differentiation. *Nat Biotechnol* **28**:511–515. <https://doi.org/10.1038/nbt.1621>.
38. Wang X, Matsumoto H, Zhao X, Das SK, Paria BC. 2004. Embryonic signals direct the formation of tight junctional permeability barrier in the decidualizing stroma during embryo implantation. *J Cell Sci* **117**:53–62. <https://doi.org/10.1242/jcs.00826>.